Spin-Phonon Coupling in $CuGeO_3$

M. Braden,[1,2] B. Hennion,[2] W. Reichardt,[1] G. Dhalenne,[3] and A. Revcolevschi[3]
[1]*Forschungszentrum Karlsruhe, INFP, Postfach 3640, 76021 Karlsruhe, Germany*
[2]*Laboratoire Léon Brillouin, CE-Saclay, 91191 Gif-sur-Yvette, France*
[3]*Laboratoire de Chimie des Solides, Université Paris-Sud, 91405 Orsay Cedex, France*
(Received 4 November 1997)

The lattice dynamics of the spin-Peierls (SP) system $CuGeO_3$ have been analyzed by inelastic neutron scattering combined with shell model calculations. The low-lying modes of the symmetry of the structural distortion in the dimerized phase are identified and studied as a function of temperature. Surprisingly, the static distortion in the SP phase does not correspond to one eigenmode of the high symmetry phase. The two modes associated with the structural distortion exhibit frequency shifts and pronounced linewidth broadening well above the transition temperature; however, there is no soft mode behavior for these modes. [S0031-9007(98)05674-9]

PACS numbers: 75.40.Gb, 61.12.Ex, 63.20.–e

A spin-Peierls (SP) transition results from spin-lattice coupling and, hence, should lead to peculiarities in the magnetic as well as in the lattice properties. Concerning the lattice dynamics in the SP compound $CuGeO_3$ (CGO) [1], infrared and Raman studies determined almost all optical Γ-point frequencies [2]; however, any dimerization must be related to modes away from the zone center, which can be investigated only by neutron scattering. Several neutron studies have focused on the acoustic branches [3–5] revealing a particularly low LA branch along the b axis whose relevance for the spin-phonon coupling still needs to be clarified. The search for a soft mode related to the structural distortion at the SP transition has so far remained unsuccessful. Answering whether the associated phonon mode softens at T_{SP} or not, is, however, essential for the understanding of the underlying mechanism.

Additional information on the lattice dynamics was obtained by optical techniques in the distorted phase, where the high-symmetry zone boundary (0.5 0 0.5) is folded into a new zone center, and where new optical active phonon modes should appear. Indeed, several groups have reported new Raman scattering peaks below T_{SP} [6–13], at $\sim$1, 3.2, 6.8, 11.1, and 24.6 THz. However, there is controversy about the interpretation of these intensities. There seems to be agreement on the facts that the lowest peak has a magnetic origin [6–14], and that the two highest frequencies are due to phonons. The 6.8 THz feature is commonly assumed to have a magnetic origin [6–13] and the one at 3.2 THz is interpreted as either magnetic [6,7] or phononic [8,10]. We will show by combining inelastic neutron scattering results with lattice dynamical model calculations that the four intensities correspond to the frequencies of the four phonon modes of the same symmetry as the distortion below T_{SP}. However, none of these modes shows an indication of softening at the SP transition.

The inelastic neutron scattering experiments were performed on the triple axis spectrometers 2T and 1T installed at the Orphée reactor. Double focusing crystals were used as monochromator [pyrolytic graphite (PG) (002) and Cu-(111)] and analyzer [PG-(002)]. Two crystals of about 600 mm^3 volume each were coaligned for measurements in the (010) geometry; for other scattering planes only one of them having a small mosaic spread [15] was used. The occurrence of the SP transition in these crystals was verified by studying the superstructure peaks.

A first description of the lattice dynamics can be obtained from the optical data determining the phonon frequencies at the zone boundary [2], where the high symmetry is reflected by the decomposition into eight distinct representations. However, the strong dispersion and the mixing of the branches along all directions necessitate more detailed information on the mode frequencies in the entire zone. Therefore, we have determined an almost complete set of dispersion curves along the orthorhombic directions at room temperature. In this Letter we focus on the $[x0x]$ direction since the structural distortion in the SP phase occurs at the zone boundary in this direction. According to the low symmetry of the $[x0x]$ line, the 30 branches decompose corresponding to two irreducible representations including 17 and 13 branches, respectively; experimental and calculated results are shown in Fig. 1 for the branches belonging to the second irreducible representation along $[x0x]$.

The lattice dynamical model was obtained by fitting its parameters to the zone-center frequencies obtained by optical techniques [2] and to the frequencies obtained by our neutron scattering experiments. The entire data set consists of about 700 observations, which are reproduced with an averaged difference of 0.2 THz. The model incorporates different types of interactions reflecting the ionic and the covalent characters of the bonds. Short range forces are described by Born-Mayer potentials and some force constants. The mainly covalent Ge-O bonds require the introduction of angular forces. Coulomb potentials and isotropic core shell interactions reflect the ionic character. In addition to the fitting of the phonon frequencies, it was verified that the model describes the neutron scattering

 0031-9007/98/80(16)/3634(4)$15.00

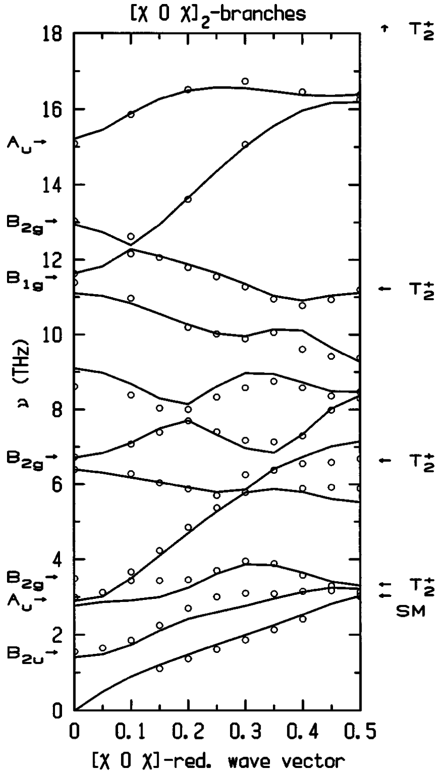

FIG. 1. Low frequency part of the phonon dispersion along [101] at room temperature; only branches belonging to the second irreducible representation are shown. The symbols denote the experimental data and the lines the frequencies calculated by a shell model.

intensities correctly. The final agreement between calculated structure factors and experimental intensities ascertains that the calculated elongation patterns are reliable. The model parameters can be obtained in Ref. [16].

The dispersion of the branches along [101] shown in Fig. 1 exhibits pronounced slopes and complicated interactions. There is a $[x0x]_2$ branch which exhibits softening when approaching (0.5 0 0.5); its zone-boundary frequency is indicated by the symbol SM in Fig. 1. This indication of a structural instability can be well reproduced by our lattice dynamical model; the analysis of the elongation pattern reveals, however, that it is not related to the SP transition.

The structural distortion in CGO in the dimerized phase is characterized by two elements [17,18]: the first consists of a Cu shift parallel to c accompanied by a modulation of the O2-O2 edge lengths perpendicular to c (O2 denotes the oxygen site closer to the Cu atoms and O1 the other), and the second element corresponds to a twisting of the CuO_2 ribbons around the c axis. Some of these features can be found in the polarization patterns of the Γ modes. The A_u mode with a frequency at 3 THz corresponds to vibrations of the Cu atoms along c; following the branch starting at A_u the pure elongation pattern is rapidly lost due to mixing with oxygen displacements. The second element of the structural distortion is related to a Γ mode, where the entire ribbons are rotated; it can be identified as the B_{2g} mode near 3.5 THz. The branch starting at B_{2g} shows a flat dispersion along $[x0x]$ indicating only weak coupling for this distortion along a and c.

At the zone boundary, the higher symmetry yields a decomposition of the modes according to eight irreducible representations. Group theory shows that the symmetry reduction of the structural part of the SP transition, from *Pbmm* to *Bbcm*, corresponds to an irreducible representation with a multiplicity of 4, T_2^+ in the notation of Ref. [19]. These modes are characterized by a Cu displacement along c, an O2 shift along a and b, and a Ge displacement along b, i.e., the additional free atomic parameters in the *Bbcm* phase [18]. For an usual structural phase transition one expects that the static distortion below the transition corresponds to the polarization of one eigenmode, whose frequency should soften close to zero in the case of a continuous displacive transition. In $CuGeO_3$ this picture does not apply for the polarization patterns of the eigenmodes; see Table I. It is obvious that the condensing static distortion corresponds to the superposition of at least the two modes with the lower frequencies. Approximately, one obtains the observed distortion by adding the polarization vectors of the lowest and second lowest modes with weighting factors of 2 and 3, respectively. Although the polarization vectors may slightly vary with the model parameters, it can be excluded that the distortion corresponds to one mode. For instance, the two low-lying modes have opposite and strong Ge displacements, whereas the static distortion exhibits only a negligible Ge shift [18]. Furthermore, only the 6.8 THz mode involves appreciable Cu displacement, which is essential for the dimerization. The 3.3 THz mode is associated with the twisting of the CuO_2 ribbons, forming the second element in the distortion. The fact that the spin system is intimately coupled to two distinct modes has to be taken into account in any quantitative theory.

The alternation of J due to the structural distortion is caused mainly by the modulation of the bond angles. The strongest influence is found for the Cu-O2-Cu bond angle, η, which is close to 90° for which value, in the absence of sidegroups, the interaction should be ferromagnetic, as has been discussed in detail in Refs. [18,20]. The deviation

TABLE I. Polarization schemes (calculated by our shell model) and frequencies of the four T_2^+ modes of the symmetry of the SP distortion. The eigenvector components are given in relative units. For comparison, the last column shows the components of the static distortion in the SP phase [18] in 0.01 Å.

T_2^+ modes	a	b	c	d	SP
Cu(0.5 0 0)z	0.11	0.72	0.51	0.00	0.57
Ge(0.07 0.25 0.25)y	0.26	−0.39	0.50	−0.44	0.08
O2(0.28 0.08 0.5)x	0.80	0.35	−0.66	−0.60	−0.95
O2-y	−0.86	0.22	−0.14	−0.86	−0.65
ν Neutron (THz)	⋯	11.4	6.8	3.3	⋯
Raman (THz)	24.6	11.1	6.9	3.2	⋯

of η from 90° induces the main anti-ferromagnetic contribution and the modulation of η in the distorted phase can explain a large splitting of J. The 6.8 THz mode corresponds to the maximum change of this angle as the Cu is shifted towards the elongating O2-O2 edge; in contrast, the Cu-O distance is only slightly changed in this mode; see Table I. Therefore, one expects a particularly strong coupling for this η-modulating mode near 6.8 THz.

The associated mode in which the Cu and O2 displacements have opposite phases modulates only slightly the bond angle but strongly the bond distance. As a consequence, its frequency is higher, 11.4 THz. This mode should not couple to the dimerization and, indeed, this polarization pattern does not seem to contribute to the SP distortion. Furthermore, this mode shows no temperature dependency, neither in frequency nor in width.

The second structural element rendering the magnetic interaction in $CuGeO_3$ antiferromagnetic consists of a hybridization between the Ge and the O2's [18,20]. The Ge is not located in the plane formed by the CuO_2 ribbons, where the effect for J should be maximal, but the angle O2-O2-Ge, δ, amounts to about 20°. The modulation of this angle will change the hybridization and hence J; however, as this contribution is close to its maximum, the angular dependence should be lower: Geertsma and Khomskii proposed this element to be the main mechanism for the alternation of J [20]. The low-lying mode near 3.3 THz corresponds to the maximum modulation of δ, see Table I, and might be coupled to the spin system via this mechanism.

The fourth T_2^+ mode has almost ideal Ge-O bond stretching character and, hence, a high frequency, which prevented a determination by neutron scattering until now.

After the identification of the relevant modes, temperature-dependent measurements were undertaken. Unfortunately, frequencies of the two low-lying T_2^+ modes are close to those of other phonons; see Fig. 2. At room temperature both T_2^+ modes appear slightly broadened in respect to the resolution, which is seen in the neighboring peaks. Upon cooling, the shape of the scans across the lower frequency phonon group is changing; see left part of Fig. 2. The T_2^+ mode near 3.3 THz significantly hardens upon cooling; see Fig. 3. This temperature dependency is more pronounced at lower temperature in contrast to an usual frequency shift induced by the thermal expansion. Furthermore, the observed effect is exceptionally large. This frequency shift exhibits a striking similarity to the magnetoelastically induced structural effects [21]. It seems unquestionable to attribute the pronounced hardening to the spin-phonon coupling. Near T_{SP} no singularity is observed, and particularly there is no indication of a softening. Furthermore, this mode remains well defined near the SP transition.

The scans across the 6.8 THz phonon mode performed at (0.5 4 0.5) exhibit even more dramatic effects. At room-temperature and at 200 K, the two phonon modes

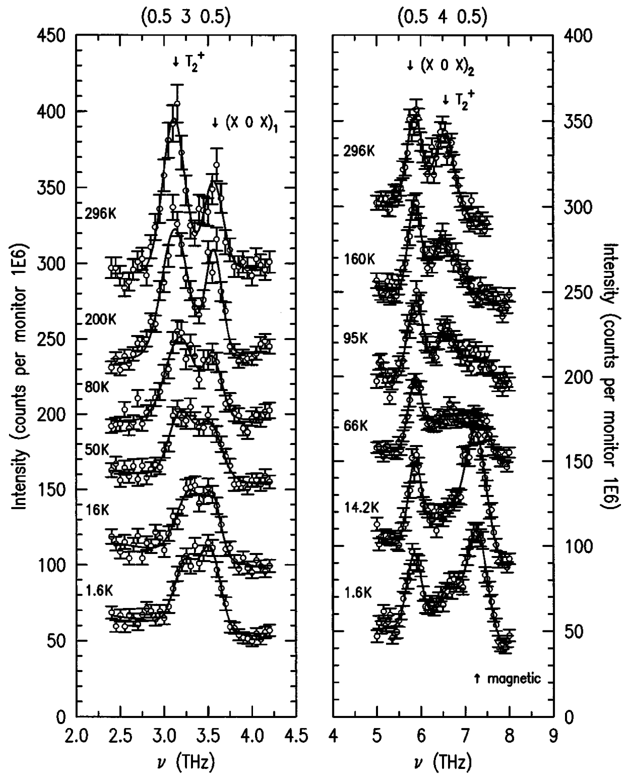

FIG. 2. Raw data scans across the two lowest T_2^+ modes as a function of temperature. The left part shows the scans across the 3.3 THz T_2^+ mode which cannot be measured separately; it is partially superposed with a mode of $(x0x)_1$ symmetry near 3.5 THz. Also the scans across the higher T_2^+ mode show a second phonon, of $(x0x)_2$ symmetry. In addition, a sharp intensity appears near 7.3 THz at low temperature.

can be separated, the T_2^+ mode being broader. This broadening becomes significantly enhanced below 160 K, where the frequency increases. At even lower temperature an additional intensity appears near 7.3 THz which becomes dominating on further cooling. Therefore, it is difficult to separate the T_2^+ mode which we observe as a shoulder on the additional intensity at low temperature. Below T_{SP}, we find a frequency of 6.76 THz for the T_2^+ mode, again indicating a pronounced shift in comparison with its 200 K value. Scans with improved resolution demonstrate that the phonon mode at 6.8 THz is broadened and the additional intensity shows a sharp profile.

The additional feature appears at the energy of the upper boundary of the magnetic excitation continuum determined by Arai *et al.* [22]. Furthermore, the ratio of its intensity with that of the well defined magnonlike low energy excitation agrees well with the intensity ratio between the upper boundary and the low-energy excitation reported in [22]. Therefore, it appears reasonable to identify the feature in Fig. 2 with the upper limit of the magnetic excitation continuum. The magnetic origin is further supported by the nonobservation of this feature at (0.5 10 0.5) where a comparably strong dynamical structure factor is calculated for the phonon mode, and where any magnetic scattering is

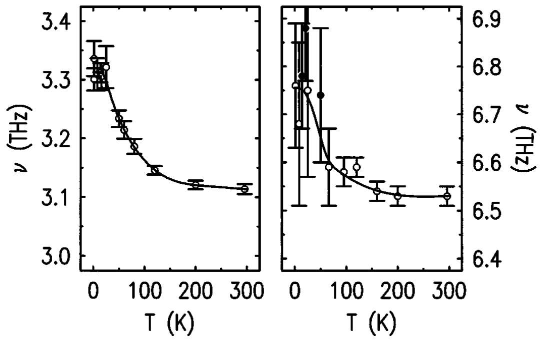

FIG. 3. Frequencies of the two lowest T_2^+ modes as a function of temperature. The values were obtained by fitting the measured intensity scans, see Fig. 2, with two or three Gaussians. Position and width of the mode at 3.5 THz were kept constant. Because of the difficulties in the determination of the 6.8 THz mode as a shoulder on the additional intensity of temperature-independent position and shape, at some temperatures, the width and position of the additional intensity was constrained (filled points). Lines are guides to the eye.

strongly suppressed due to the Cu^{2+} magnetic form factor. Recent calculations of the neutron scattering function indeed predict a sharp peak near the upper boundary of the two-spinon continuum for strong next nearest neighbor frustration [23].

The three low temperature frequencies attributed to the T_2^+ modes can be compared to the additional peaks appearing in Raman scattering [6–13]; see Table I. In the SP phase, (0.5 0 0.5) is folded to the zone center and the former T_2^+ modes have A_g symmetry, i.e., the full symmetry of the *Bbcm* phase, and are Raman active. The frequencies of the intermediate three new peaks agree nicely with our results. Therefore, it seems most likely that all these peaks have, at least partially, a phononic origin in contrast with previous interpretations. The two lowest peaks, at 3.2 and 6.8 THz, are strongly asymmetric and broad in the Raman spectra; they can be well described by a Fano line shape confirming the strong coupling to the magnetic excitations [8,24]. Especially the 6.8 THz mode exhibits a very large linewidth, close to the one observed in our neutron scattering experiment.

The existence of two structural order parameters corresponding to two phonon modes of rather high frequency indicates a mechanism distinct from the conventional theory, which is based on phonon softening [25]. The most anomalous behavior of the 6.8 THz mode, which is observed in neutron as well as in Raman scattering, further demonstrates that its associated distortion scheme, i.e., the modulation of the Cu-O2-Cu bond angle, is strongly coupled to the magnetism, in agreement with the calculation in Ref. [18]. It, therefore, seems likely that this element contributes most to the alternation of J in the dimerized phase. The change of the Ge-O hybridization, associated with the 3.2 THz mode, experiences spin-phonon coupling too, however, to a smaller extent.

The nonexistence of phonon softening at T_{SP} for the associated modes appears surprising at first sight. However, both involved phonons have frequencies much higher than the magnetic gap opening at T_{SP}. These modes experience the magnetoelastic coupling upon cooling below J/k_b as clearly demonstrated by the data, while they remain unaffected by the small change in the magnetic excitation spectrum at T_{SP}.

We are grateful to G. Güntherodt, P. Lemmens, U. Loew, J. Lorenzana, P. van Loosdrecht, and G. Uhrig for several stimulating discussions.

[1] M. Hase *et al.*, Phys. Rev. Lett. **70**, 3651 (1993).
[2] Z. V. Popovic *et al.*, Phys. Rev. B **52**, 4185 (1995).
[3] J. E. Lorenzo *et al.*, Phys. Rev. B **50**, 1278 (1994).
[4] K. Hirota *et al.*, Physica (Amsterdam) **213B–214B**, 284 (1995).
[5] M. Nishi *et al.*, Physica (Amsterdam) **210B**, 149 (1995).
[6] M. Udagawa *et al.*, J. Phys. Soc. Jpn. **63**, 4060 (1994).
[7] H. Kuroe *et al.*, Phys. Rev. B **50**, 16 468 (1994).
[8] P. H. M. van Loosdrecht *et al.*, Phys. Rev. Lett. **76**, 311 (1996).
[9] H. Kuroe *et al.*, Physica (Amsterdam) **219B–220B**, 104 (1996).
[10] I. Loa *et al.*, Solid State Commun. **99**, 2331 (1996).
[11] N. Ogita *et al.*, Physica (Amsterdam) **219B–220B**, 107 (1996).
[12] P. Lemmens *et al.*, Physica (Amsterdam) **223B–224B**, 535 (1996).
[13] V. N. Muthukumar *et al.*, Phys. Rev. B **55**, 5944 (1997).
[14] C. Gros *et al.*, Phys. Rev. B **55**, 15 048 (1997); W. Brenig, Phys. Rev. B **56**, 2551 (1997).
[15] G. Dhalenne *et al.*, MRS Bull. **32**, 7939 (1997); A. Revcolevschi and G. Dhalenne, Adv. Mater. **5**, 9657 (1994).
[16] See AIP Document No. E-PAPS: E-PRLTA-80-062812 for shell-model parameter values. E-PAPS document files may be retrieved free of charge from our FTP server (http://www.aip.org/epaps/epaps.html) or from ftp.aip.org in the directory /epaps/. For further information, email: paps@aip.org; or fax: 516-576-2223.
[17] K. Hirota *et al.*, Phys. Rev. Lett. **73**, 736 (1994).
[18] M. Braden *et al.*, Phys. Rev. B **54**, 1105 (1996).
[19] H. T. Stokes and D. M. Hatch, *Isotropy Subgroups of the 230 Crystallographic Space Groups* (World Scientific, Singapore, 1988).
[20] W. Geertsma *et al.*, Phys. Rev. B **54**, 3011 (1996).
[21] M. Braden *et al.*, Phys. Rev. B (to be published).
[22] M. Arai *et al.*, Phys. Rev. Lett. **77**, 3649 (1996).
[23] K. Fabrizius *et al.*, Phys. Rev. B **55**, 5833 (1997); K. Fabrizius *et al.*, report.
[24] P. H. M. van Loosdrecht (private communication).
[25] M. C. Cross and D. S. Fisher, Phys. Rev. B **19**, 402 (1979).